Biomedicine & Pharmacotherapy 192 (2025) 118657

Contents lists available at ScienceDirect

Biomedicine & Pharmacotherapy

journal homepage: www.elsevier.com/locate/biopha

Aloe-derived polysaccharides (APS) mitigate SARS-CoV-2 Omicron BQ1.1 infection by preserving epithelial integrity and reducing viral load in human airway epithelial (HAE) cultures

Wilfried Posch [a,1], Ekambaranellore Prakash [b,1], Sophie Ann Erckert [a], Viktoria Zaderer [a], Rosa Bellmann-Weiler [c], Uvarani Chokkalingam [b], Singh Anuma [b], Stefan Pöhlmann [d], Markus Hoffmann [d], Doris Wilflingseder [e,*]

[a] Institute of Hygiene and Medical Microbiology, Medical University of Innsbruck, 6020, Austria
[b] Dazzeon Biotech Co., Ltd., Wuquan 1st road, Xinzhuang district, New Taipei City 242, Taiwan
[c] Department of Internal Medicine II, Medical University of Innsbruck, Anichstraße 35, Innsbruck, Austria
[d] Infection Biology Unit, German Primate Center - Leibniz Institute for Primate Research, Göttingen, Germany
[e] The Ignaz Semmelweis Institute, Interuniversity Institute for Infection Research, University of Veterinary Medicine Vienna, Vienna 1210, Austria

ARTICLE INFO

Keywords:
Aloe vera
Polysaccharides
SARS-CoV-2
Human Airway Model
Innate immunity
Antiviral prophylaxis

ABSTRACT

Aloe-derived polysaccharides (APS) show promising antiviral activity against the SARS-CoV-2 Omicron variant BQ1.1, offering a potential new line of defense for the respiratory epithelium. Recently, two APS formulations, A50 and I50, differing in molecular weight and acetylation, yet sharing a structural backbone like acemannan were characterized. The two compounds were tested in monolayer and pseudostratified human airway epithelial (HAE) cultures and notably, both compounds demonstrated minimal cytotoxicity and low innate immune activation, highlighting their safety profile. When applied topically 30 min before infection in differentiated HAE cells, APS significantly strengthened epithelial barrier integrity, as shown by increased transepithelial electrical resistance (TEER). Viral RNA levels were markedly reduced on both the apical and basolateral surfaces, and viral plaque assays confirmed decreased viral spread. Together, these findings position APS as promising prophylactic agents capable of reinforcing epithelial defenses and limiting SARS-CoV-2 infection, thus offering broad potential against current and emerging respiratory viral threats.

1. Introduction

The respiratory epithelium is constantly challenged by various pathogens, allergens and inhaled toxins from the environment [1,2], which can lead to infection and chronic airway diseases [3]. Epithelial integrity orchestrated by tight and adherens junctions [4], is often compromised in patients with respiratory viral infections, increasing the risk of severe disease and mortality [5,6]. Severe Acute Respiratory Syndrome Coronavirus 2 (SARS-CoV-2), the causative agent of the COVID-19 pandemic, has challenged global public health due to its high transmissibility and the emergence of multiple variants of concern/interest (VoCs/VoIs) [7,8]. Although it can infect individuals of all ages, those with compromised immune systems are particularly vulnerable to severe outcomes [9]. Upon infection, SARS-CoV-2 perturbs epithelial tight and adherens junctions, redistributes ZO-1, decreases mucociliary clearance, and increases paracellular permeability [10–13], thereby weakening the epithelial barrier, facilitating viral dissemination, and amplifying inflammatory responses [14–16]. Preserving epithelial integrity is therefore critical for limiting viral spread and preventing the hyper-inflammatory states characteristic of severe COVID-19.Due to the emergence of multiple VoCs/VoIs with different characteristics, developing a rapid, easy-to-use and broadly effective preventive measures, such as antiviral treatments, are needed to mitigate the risk of severe respiratory diseases.

Several plant-derived compounds are known for their beneficial effects on epithelial cells [17–20]. In particular, polysaccharides can

* Correspondence to: The Semmelweis Institute, Interuniversity Institute for Infection Research, University of Veterinary Medicine Vienna, Veterinärplatz 1, Vienna 1210, Austria.
E-mail address: doris.wilflingseder@vetmeduni.ac.at (D. Wilflingseder).
[1] equal contribution

https://doi.org/10.1016/j.biopha.2025.118657
Received 10 June 2025; Received in revised form 8 October 2025; Accepted 16 October 2025
Available online 21 October 2025

safeguard epithelial integrity against infections and environmental insults, while also providing anti-inflammatory and antioxidant benefits [21,22] and may offer therapeutic benefits against COVID-19 [23]. Aloe vera (*Aloe barbadensis* Miller), a rich source of polysaccharides, is renowned for its diverse biological attributes, including antiviral properties [24]. Commonly known as acemannan (acetylated mannan), Aloe-derived polysaccharide (APS) has been commercially utilized for various health and personal care applications [25,26]. Here, we report the effects of APS, A50 and I50 [27], with varying acemannan and acetylation contents on epithelial barrier function, inflammatory reactions, viral load reduction and infectivity of SARS-CoV-2-infected highly differentiated human respiratory epithelial cells in air-liquid-interphase (ALI) model. Our data emphasize the role of APS in protecting barrier integrity, rather than exerting direct antiviral effects.

2. Materials and methods

2.1. Isolation and characterization of APS - A50 and I50

Polysaccharide fractions were separated from *Aloe* gel using a patented fractionation technology (US 2022/0072080 A1) as described in Shih et al. [28]. Both A50 and I50 were further characterized using Attenuated Total Reflectance-Fourier Transform Infrared spectrometer (ATR-FTIR, Thermo Scientific Nicolet™ iS™ 5), Nuclear magnetic resonance (NMR, Bruker AVANCE III HD 600 MHz), and High-performance liquid chromatography (HPLC, Agilent 1260-Infinity II Prime LC, Agilent Technologies) [28].

2.2. Cell viability assay using Vero/Calu-3 cells

On day 0, Vero cells (ATCC Cat# CRL-1586; RRID: CVCL_0574) and Calu-3 cells (ATCC Cat# HTB-55; RRID: CVCL_0609) were seeded in 96-well plates. On day 1, the culture medium was aspirated and 50 µl of compound dilutions were added (starting at 10 mg/ml [undiluted]). Cells treated with culture medium without compound served as control. After 30 mins incubation at 37 °C and 5 % CO_2, 50 µl of fresh medium was added and cells were incubated for another 18 h. On day 2, cell viability was measured using the CellTiter-Glo® Luminescent Cell Viability Assay (Promega, Cat# G7570). 100 µl of substrate were added per well, incubated for 10 min at room temperature in the dark, then transferred into white 96-well plates for luminescence measurement using Hidex Sense Plate luminometer. The assay was performed three times, each with technical quadruplicates.

2.3. Inhibition assays using Vero/Calu-3 and pseudoviruses

(A) Treatment: Cells only: On day 0, Vero cells (ATCC Cat# CRL-1586; RRID: CVCL_0574) and Calu-3 cells (ATCC Cat# HTB-55; RRID: CVCL_0609) were seeded in 96-well plates (100,000 cells/well). On day 1, the culture medium was aspirated and 50 µl of compound dilutions were added (2.5 mg/ml, 0.625, to 0.0098 mg/ml). Cells treated with culture medium without compound served as control. After 30 min incubation at 37 °C and 5 % CO_2, the supernatant was aspirated and 50 µl of fresh medium added, followed by 50 µl of pseudovirus. Cells were incubated for 18 h and firefly luciferase activity was measured using the Beetle-Juice Kit, PJK, (Cat# 102511) in a Hidex sense plate luminometer. The assay was performed three times and each with technical quadruplicates.

(B) Treatment: Cells and pseudovirus: On day 0, Vero cells (ATCC Cat# CRL-1586; RRID: CVCL_0574) and Calu-3 cells (ATCC Cat# HTB-55; RRID: CVCL_0609) were seeded in 96-well plates (100,000 cells/well). On day 1, the culture medium was aspirated and 50 µl of different dilutions of compound were added (2.5, 0.625, 0.15625, 0.0390625, and 0.0098 mg/ml). Medium without compound served as control. After 30 min of incubation at 37 °C and 5 % CO_2, 50 µl of pseudovirus were added. Cells were incubated for 18 h and luciferase activity was measured using the Beetle-Juice Kit, PJK, (Cat# 102511) in a Hidex sense plate luminometer. The assay was performed three times and each with technical quadruplicates.

To analyze the inhibitory activity of the compound, pseudovirus cell entry (given as luminescence counts per second) was normalized to samples without compound (= 100 % pseudovirus entry) using Microsoft Excel. The normalized data were further processed using GraphPad Prism to generate the data graphs.

2.4. NHBE cell culture

Normal human bronchial epithelial (NHBE, Lonza, cat# CC-2540 S, Germany) cells are available in our laboratory and are routinely cultured at the air-liquid interface (ALI) as described in previous studies [29–31]. Briefly, the cells were cultured in a T75 flask for 3 days until they reached 80 % confluency. Cells were then detached using TrypLE (Thermo Fisher Scientific) and seeded onto GrowDexT (UPM)-coated 0.33 cm^2 porous (0.4 µm) polyester membrane inserts at a density of 1×10^5 cells per Transwell (Costar, Corning, New York, NY, USA). The cells were grown to near confluency in submerged culture for 2–3 days in specific epithelial cell growth medium as per the manufacturer's instructions (PneumaCult™-Ex Plus Medium, Stemcell, cat# 05040, Germany). Cultures were maintained in a humidified atmosphere with 5 % CO_2 at 37 °C and then transferred to ALI culture in PneumaCult™-ALI medium (Stemcell, cat# 05001, Germany) for an additional 30 days until fully differentiated.

2.5. Pseudovirus production

Vesicular stomatitis virus-derived pseudoviruses bearing the glycoprotein of vesicular stomatitis virus (VSV-G) or the spike (S) protein of SARS-CoV-2 (PANGO lineage B.1, GISAID-identifier: EPI_ISL_425259) were produced as follows: On day 0, HEK-293T cells (DSMZ, Cat# ACC-635; RRID: CVCL_0063) were seeded in 6-well plates (250,000 cells/well) and incubated for 24 h at 37 °C and 5 % CO_2. On day 1, cells were transfected with expression plasmid for VSV-G or SARS-2-S (8 µg/well) via calcium-phosphate transfection method and further incubated for 16 h at 37 °C and 5 % CO_2. Cells transfected with empty plasmid or DsRed expression plasmid served as controls. On day 3, cells were inoculated with VSV-G-transcomplemented VSV*ΔG (a replication-restricted vesicular stomatitis virus that lacks the genetic information for VSV-G but instead codes for two reporter proteins, eGFP and firefly luciferase) at a multiplicity of infection of 3 and incubated for 1 h at 37 °C and 5 % CO_2. Thereafter, the inoculum was removed and cells were washed with PBS, before medium containing anti-VSV-G antibody (I1, produced from CRL-2700 mouse hybridoma cells; ATCC, Cat# CRL-2700; RRID: CVCL_G654) was added and cells were further incubated for 18 h at 37 °C and 5 % CO_2 (of note, cells expressing VSV-G received medium without anti-VSV-G antibody). On day 4, supernatants were collected, centrifuged (2000 x g, 4 °C, 10–15 min; to remove cellular debris), aliquoted and stored at −80 °C.

2.6. Viruses

Clinical specimens for SARS-CoV-2 Omicron BQ1.1 from COVID-19-positive swabs, sequenced by the Austrian Agency for Health and Food Safety, Vienna, Austria were propagated in Vero cells and subsequently used to infect cells.

2.7. Vero cells

The VeroE6/TMPRSS2/ACE2 cell line used was a modified version of VeroE6 cells that express elevated levels of TMPRSS2 and ACE2, making it highly susceptible to SARS-CoV-2 infection. It was acquired through the CFAR (NIBSC) and was described by Matsuyama et al. [32]. This cell line was utilized to cultivate well-characterized wild-type (WT) and

BA.5 variants of the virus from patient samples.

2.8. Immunofluorescence (IF) analyses

For visualization of APS effects on 3D tissue models, cells were incubated with various concentrations of A50 and I50. After SARS-CoV-2 exposure, 3D cell cultures were fixed with 4 % paraformaldehyde. Intracellular staining was performed using 1X Intracellular Staining Permeabilization Wash Buffer (10X; BioLegend, San Diego, CA, USA). Nuclei were detected using Hoechst 33342 (Cell Signaling Technologies, cat# 4082, Netherlands), complement C3 using a C3-FITC (Agilent Technologies, cat# F020102–2, Austria) and cilia using an acetylated Tubulin-Alexa647 antibody (Abcam, cat# ab218591, UK). After staining, 3D cultures were mounted in Mowiol. To study these complex models using primary cells cultured in 3D and to generate detailed phenotypic fingerprints for deeper biological insights, the Operetta CLS System (PerkinElmer, Waltham, MA, USA) was used. Harmony™ Software was used and analyses performed in more than 1500 cells per condition.

2.9. Transepithelial electrical resistance (TEER) measurements

To monitor epithelial integrity, 3D NHBE cultures were maintained upon treatment, samples were added to the apical side of the epithelium prior infection with the Omicron BQ1.1 variant. Transepithelial electrical resistance (TEER) was measured several days post infection (dpi) (1, 2, 3 dpi). TEER values were measured using EVOM voltohmeter with STX-2 chopstick electrodes (World Precision Instruments, Stevenage, UK). For measurements, 0.1 ml and 0.7 ml of medium were added to the apical and basolateral chambers, respectively. Cells were allowed to equilibrate before TEER was measured. TEER values reported were corrected for the resistance and surface area of the Transwell filters.

2.10. Real-time RT-PCR for viral load analysis

SARS-CoV-2 was extracted using FavorPrep Viral RNA Mini Kit, according to manufacturer's instructions (Favorgen Europe, cat# FAVRE 96,004, Austria). Sequences specific to 2 distinct regions of the Nucleocapsid (N) gene, N1 and N2, for SARS-CoV-2, were used. The Luna Universal Probe One-Step RT-qPCR Kit (New England Biolabs, cat# E3006, Germany) was used to quantify the virus using absolute quantification and SARS-CoV-2 RNA standard control obtained from the National Institute for Biological Standards and Control, UK. All experimental runs were performed on a Bio-Rad CFX 96 instrument and analyzed by the Bio-Rad CFX Maestro 1.1 software (Bio-Rad, Germany). Samples for viral quantification were taken apically and basolaterally on several dpi.

2.11. Plaque assay for analyzing infectivity of the released virus

VeroE6/ACE2/TMPRSS2 cells were inoculated with serial dilutions of subnatants from Omicron-infected NHBE cells for 1 h at 37 °C/5 % CO_2. Inoculate was replaced with culture medium containing 1.5 % carboxymethylcellulose and incubated for 3 days at 37 °C/5 % CO_2 before plaque visualization and counting as described [29].

2.12. Statistical analysis

Statistical analysis of differences was performed utilizing the GraphPad prism software and using OneWay ANOVA with Tukey's posttest or unpaired Student's *t* test upon comparison of two groups.

3. Results

3.1. Aloe product A50 does not impact cell viability, while blocking pseudovirus entry in Vero – but not Calu – cells

We first tested A50 in Vero and Calu-3 cell lines, for cell viability and inhibition of pseudovirus entry bearing VSV-G or SARS-CoV-2 spike protein (SARS-2-S). To monitor viability, cells were incubated with A50 across a concentration range of 0.0048828–10 mg/ml, diluted in culture medium; except for 10 mg/ml stock which was used undiluted (prepared in water/0.2 % ethanol). Medium without compound served as control. Cell viability was assessed by measuring cellular adenosine triphosphate via the CellTiter-Glo® Luminescent Cell Viability Assay (Fig. 1A). A50 did not impact viability of Vero and Calu-3 cells up to 5 mg/ml, but a significant reduction (~70 %) in cell viability was observed at 10 mg/ml (Fig. 1A). Hence 1.5 mg/ml A50 was chosen for the analysis of cell entry driven by the SARS-CoV-2 spike protein, using two different set ups (Figs. 1B and 1C). In the set-up shown in Fig. 1B, inhibition of SARS-CoV-2 spike protein-driven cell entry was evaluated by blocking cellular factors. For this, Vero and Calu-3 cells were pre-incubated with varying compound concentrations (0.0098–2.5 mg/ml), while control cells only received culture medium. After incubation the medium was replaced with fresh medium containing pseudovirus particles bearing either vesicular stomatitis virus glycoprotein (VSV-G) or SARS-CoV-2 spike protein (SARS-2-S). Under conditions where only target cells were exposed to the compound, no inhibition of SARS-CoV-2 spike or VSV-G protein mediated entry was observed (Fig. 1B). In Fig. 1C both target cells (Vero and Calu-3) and pseudovirus particles were exposed to varying concentrations (0.0098–2.5 mg/ml). No inhibitory effect was seen in Calu-3 cells, but in Vero cells, entry of pseudoviruses bearing SARS-CoV-2 spike and VSV-G was significantly and dose dependently inhibited at 0.625 and 2.5 mg/ml. Overall, A50 showed little to no cytotoxicity up to 5 mg/ml and significantly inhibited viral entry in to Vero cells, when both cells and viruses were exposed to higher compound concentrations.

3.2. Aloe products A50 and I50 exhibit little cytotoxicity in primary human cells

Following pseudovirus and cell line testing, A50 and a second compound I50 - differing in acemannan and acetylation content - were evaluated in primary airway and epithelial cell monolayers. After detailed chemical characterization [28], cytotoxicity was assessed on normal human bronchial epithelial (NHBE) cells using various assays (Figs. 2A to 2C). NHBE monolayers (90–100 % confluent) were treated with A50 (0.075–10 mg/ml) and I50 (0.625–5 mg/mlL) followed by immunofluorescence (IF) using Draq5 (Nuclei) and GhostDye510 (dead cells) (Fig. 2A). Only the highest concentration of I50 dose (5 mg/ml) showed notable cytotoxic effect; lower doses (< 2.5 mg/ml) showed minimal cell death (Fig. 2A). In 3D ALI cultures, both compounds exhibited even lower cytotoxicity with LDH activity comparable to controls up to5 m g/ml. Results from 4 independent experiments using both, A50 and I50, are summarized in Fig. 2B. IF analyses of 3D tissue models (Fig. 2C) showed that 2.5 and 5 mg/ml I50 caused slight epithelial disruption and increased C3 activation, while 0.625 mg/ml I50 preserved pseudostratified architecture and showed minimal immune activation as illustrated by C3 deposition (Fig. 2C, left). This demonstrated that *Aloe* compounds exhibit minimal cytotoxic effects, especially I50 (0.625 mg/ml) protected airway epithelial cells during SARS-CoV-2 infection.

3.3. I50 protects epithelial tissues from BQ1.1-mediated destruction

Highly differentiated NHBE cells cultured for 40 days at an air-liquid interface (ALI) were pre-treated or not with A50 and I50 (0.625, 2.5 and 5 mg/ml) for 30 mins prior to infection with BQ1.1. Mock treatments at

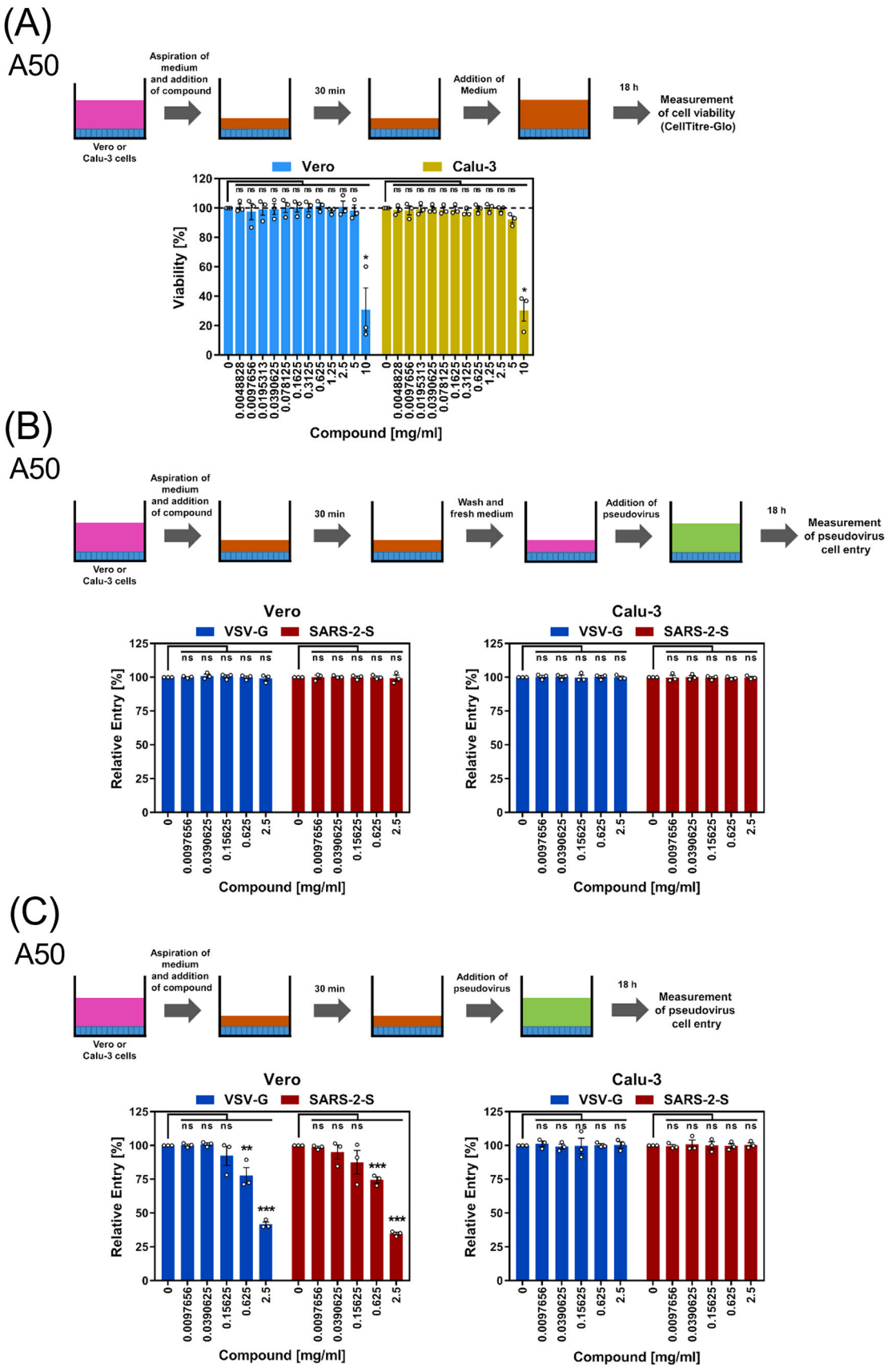

(caption on next page)

Fig. 1. Characterization of cell viability (A) and inhibitory impact (B, C) of *Aloe vera* product A50 on cell lines and using pseudoviruses. (A) Cell viability assay. Upper panel: Workflow, Lower panel: Data graph. Data represent the average (mean) cell viability obtained from N = 3 (each conducted with 4 technical replicates). Viability was normalized against cells incubated without compound. Each circle depicts one experiment. Error bars indicate the standard error of the mean. (B) Inhibition assay (Treatment: Cells only). Top: Workflow, Bottom: Data graph. Data represent the average (mean) pseudovirus cell entry obtained from 3 experiments (each conducted with 4 technical replicates). Entry was normalized against cells incubated without compound. Each circle depicts one experiment. Error bars indicate the standard error of the mean. (C) Inhibition assay (Treatment: Cells and pseudovirus). Top: Workflow, Bottom: Data graph. Data represent the average (mean) pseudovirus cell entry obtained from N = 3 (each conducted with 4 technical replicates). Entry was normalized against cell incubated without compound. Each circle depicts one experiment. Error bars indicate the standard error of the mean.

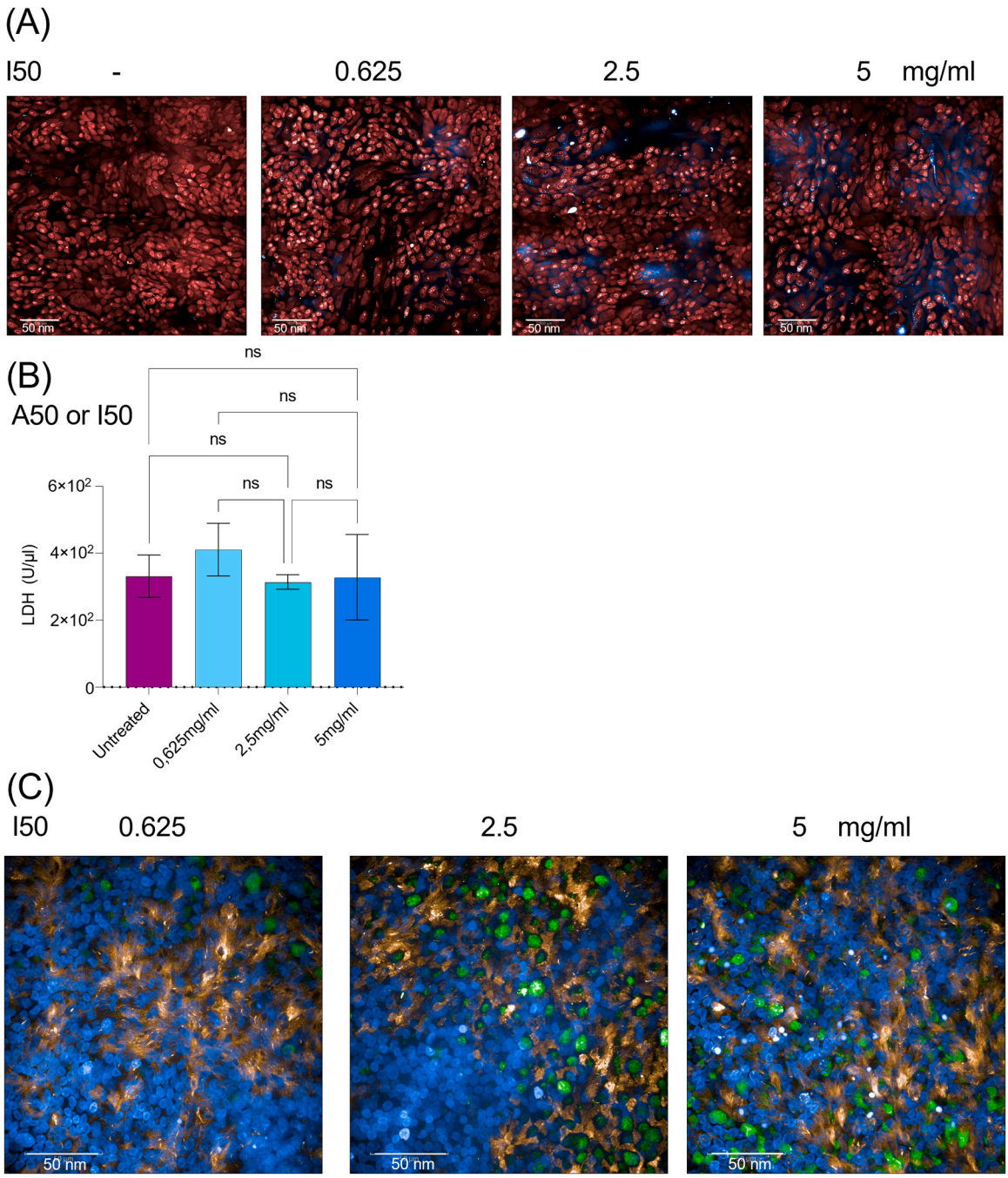

Fig. 2. Characterization of cytotoxic effects of *Aloe vera* products on NHBE cells. (A) Cytotoxicity of various concentrations of I50 were tested on NHBE monolayers. N = 3. (B) LDH release from NHBE cells are illustrated after treatment with A50 or I50. Since values did not differ on whether cells were treated with A50 or I50, a summary of 4 independent experiments each using both, A50 or I50, is depicted. Differences were analyzed using One-way ANOVA and Šidák`s multiple comparisons test. (C) Effects on various concentrations of I50 (0.625, 2.5, 5 mg/ml) on HAE tissue cultures in ALI are illustrated. Nuclei are shown in blue, cilia in orange, local complement C3 activation in green. Bars = 50 nm.

the same three concentrations served as controls. TEER was measured at multiple days post infection (dpi). As previously reported BQ1.1 caused significant TEER loss by 2 dpi (Figs. 3A and 3B). A50 at 0.625 and 2.5 mg/ml partly rescued tissue integrity while 5 mg/ml A50, had no protective effect likely due to higher cytotoxicity (Fig. 3A). Contrary to data obtained with A50, I50 significantly protected NHBE tissues from BQ1.1-mediated destruction at all concentrations tested (0.625–5 mg/ml) and illustrated similar TEER values as mock-treated, uninfected tissues, even on 2 dpi (Fig. 3B). These results show that I50 and to a lesser extent A50 could protect the respiratory epithelial barrier from BQ1.1-induced tissue damage.

3.4. Both - A50 and I50 - significantly decrease SARS-CoV-2 viral loads and infectivity

To assess efficiency of A50 and I50 in lowering release of infectious virus particles, viral loads from apical and basolateral supernatants were determined using real-time RT-PCR (Figs. 4A and 4B). Virus copy numbers in A50 (Fig. 4A)- and I50 (Fig. 4B)-treated and infected supernatants were – as expected – above mock-treated UI controls but significantly lower compared to Omicron-infected cultures (Figs. 4A and 4B). I50-pretreatment significantly reduced viral loads in both, apical (Fig. 4B, left) and basolateral (Fig. 4B, right), supernatants, while A50 also lowered viral loads, with 0.625 mg/ml being most potent in reducing apical release (Fig. 4A, left). Basolateral viral secretion was consistent across A50 concentrations (Fig. 4A, right). To determine, on whether APS prevent infection by maintaining epithelial barrier integrity or directly inhibiting viral entry / replication, we pre-incubated virus (BQ1.1) with various concentrations of A50 or I50 prior infection. These analyses revealed a minor reduction in virus copy numbers compared to mock-treated virus (INF), when BQ1.1 was pre-treated with both, A50 or I50 (Suppl. Figure 1). Given I50's superior activity, we tested the infectivity of virus particles released from NHBE cells in a plaque assay using 0.625 and 5 mg/ml. BQ1.1 supernatants. These experiments revealed a high infectivity of BQ1.1 supernatants, while plaque formation was significantly reduced by I50 pretreatment (Figs. 5A and 5B). Fig. 5A presents a representative trial, while Fig. 5B summarizes data experiments. Overall, I50 spray treatment especially at 0.625 mg/ml demonstrated strong antiviral and tissue-protective effects.

3.5. APS significantly reduces cell stress upon BQ1.1 infection

LDH analyses of 3 dpi basolateral subnatants from UI, BQ1.1-infected and APS-pretreated and infected NHBE cultures to determine virus induced cell stress and cytotoxicity. As expected, BQ.1.1 infection significantly triggered LDH release compared to UI mock-treated with various concentrations of A50 (Fig. 6A) or I50 (Fig. 6B) (0.625, 2.5, and 5 mg/ml). A significant reduction of LDH was observed in all cultures pre-treated with A50 and I50 (Figs. 6A and 6B), with – again – the lowest APS I50 concentration (0.625 mg/ml) being the most effective in decreasing virus-induced stress and cytotoxicity (Fig. 6B). Although LDH levels remained above mock controls, they were significantly lower compared to the infected condition (Figs. 6A and 6B), demonstrating that APS compounds effectively mitigate virus-induced cell stress even several days post infection (3 dpi).

4. Discussion

Airway Epithelium exerts multiple defense mechanisms to protect the host against invading pathogens and environmental toxins. Maintaining airway epithelial membrane integrity is a combinatory effect of both the barrier function and airway epithelial re-epithelization [33]. Viral infections can disrupt the airway epithelium, breach epithelial barrier function and thereby enable translocation of pathogens [34]. Polysaccharides exert anti-SARS-CoV-2 effects, in addition to their well-known anti-inflammatory properties [35–38]. Polysaccharides derived from *Aloe* showed protection against influenza viral infections [39,40] and acemannan has been shown to inhibit bacterial infections in the lung caused by *Pseudomonas* species [41,42]. While *in silico* studies

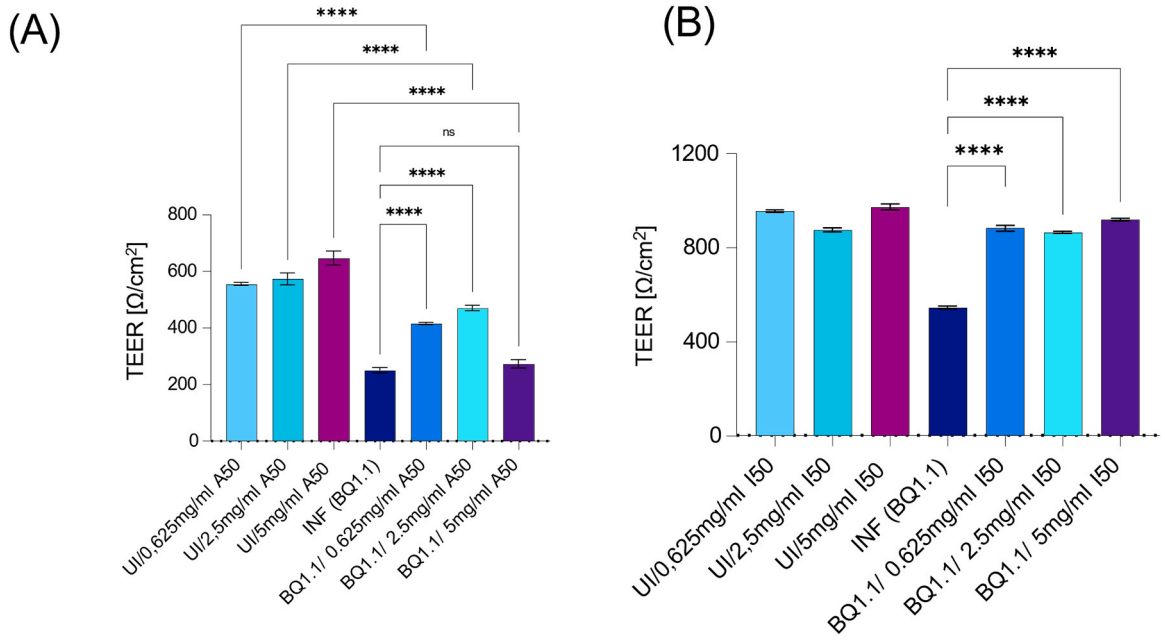

Fig. 3. Characterization of epithelial integrity of highly differentiated NHBE tissue models in ALI following infection with BQ1.1 in absence and presence of the Aloe compounds. (A) The Aloe compound A50 was applied at various concentrations (0.625–5 mg/ml) to fully differentiated NHBE cultures 30 min prior infection with BQ1.1 or not. Mock-treated controls (UI plus 0.625–5 mg/ml A50) served as controls. On 2 dpi,TEER values were measured. The experiments were repeated thrice independently. (B) The Aloe compound I50 was applied at various concentrations (0.625–5 mg/ml) to fully differentiated NHBE cultures 30 min prior infection with BQ1.1 or not. Mock-treated controls (UI plus 0.625–5 mg/ml I50) served as controls. On 2 dpi, TEER values were measured. The experiments were repeated thrice independently.

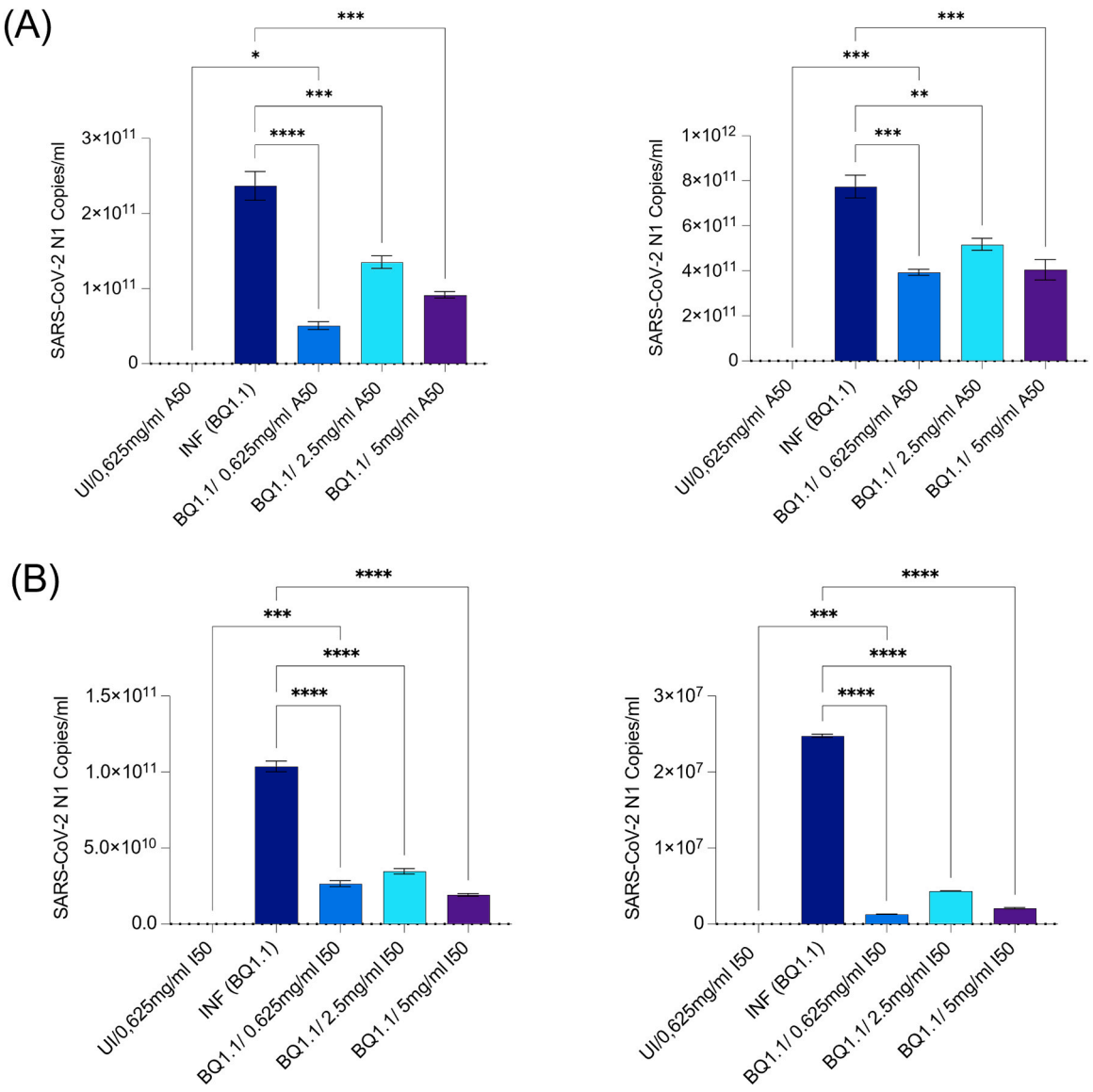

Fig. 4. Characterization of viral loads of highly differentiated NHBE tissue models in ALI following infection with BQ1.1 in absence and presence of the Aloe compounds. (A) The Aloe compound A50 was applied at various concentrations (0.625–5 mg/ml) to fully differentiated NHBE cultures 30 min prior infection with BQ1.1 or not. Mock-treated controls (UI plus 0.625 mg/ml A50) served as controls. On 3 dpi, viral loads were measured (left) apically and (right) basolaterally. Three independent experiments were analysed in duplicates. (B) The Aloe compound I50 was applied at various concentrations (0.625–5 mg/ml) to fully differentiated NHBE cultures 30 min prior infection with BQ1.1 or not. Mock-treated controls (UI plus 0.625 mg/ml I50) served as controls. On 3 dpi, viral loads were measured (left) apically and (right) basolaterally. For all analyses, three independent experiments were analysed in duplicates.

showed that *Aloe*-derived compounds primarily target SARS-CoV-2 proteases and spike protein [43,44], there is a paucity of preclinical data from live virus infection models. In the present study, A50 inhibited Vero but not Calu-3 cell entry of pseudotypes bearing the SARS-CoV-2 spike protein. This cell line-specific effect might have been due to differential dependence of Vero and Calu-3 cell entry on attachment factors like heparan sulphate or members of the TIM/TAM family, which can promote both SARS-CoV-2 spike- and VSV-G-driven entry [45–47]. Further, A50 exerted cell-protective, antiviral effects against SARS-CoV-2 infection in primary respiratory epithelial cells grown at the air liquid interface.

Both high and low molecular weight heparins including Enoxaparin have shown strong anti-SARS-CoV-2 activity via pulmonary delivery in an animal study [48] and demonstrated antiviral and anti-coagulant effects in COVID-19 patients [49,50]. Anticoagulants are widely used and considered safe with inhaled heparins not increasing plasma anti-Xa activity even at high doses [51,52]. Here, APS compounds were tested for safety using two different cell lines, primary bronchial epithelial monolayers and highly differentiated, pseudostratified HAE tissue cultures. Across a concentration range of 0.625–5 mg/ml, the compounds exhibited good safety profiles with minimal immune activation and negligible impact on epithelial integrity as confirmed by confocal microscopy.

Previous studies showed that not only Enoxaparin, but also ColdZyme®, curcumin, P80 and GlyPerA™ solution could effectively block SARS-CoV-2 variants of concern (VoCs), and in case of ColdZyme® in addition Influenza A/B or non-enveloped rhinoviruses, when used as mouth/nasal sprays, lozenges or via inhalation [24,50,53–57]. These easily accessible solutions are strong candidates for prophylactic treatment against enveloped and non-enveloped respiratory viruses. Furthermore, plant-derived medicinal products, like P80 or the two herein tested compounds, A50 and I50, are desirable for their multifaceted benefits, including low side effects, high bioavailability, and cost-effectiveness.

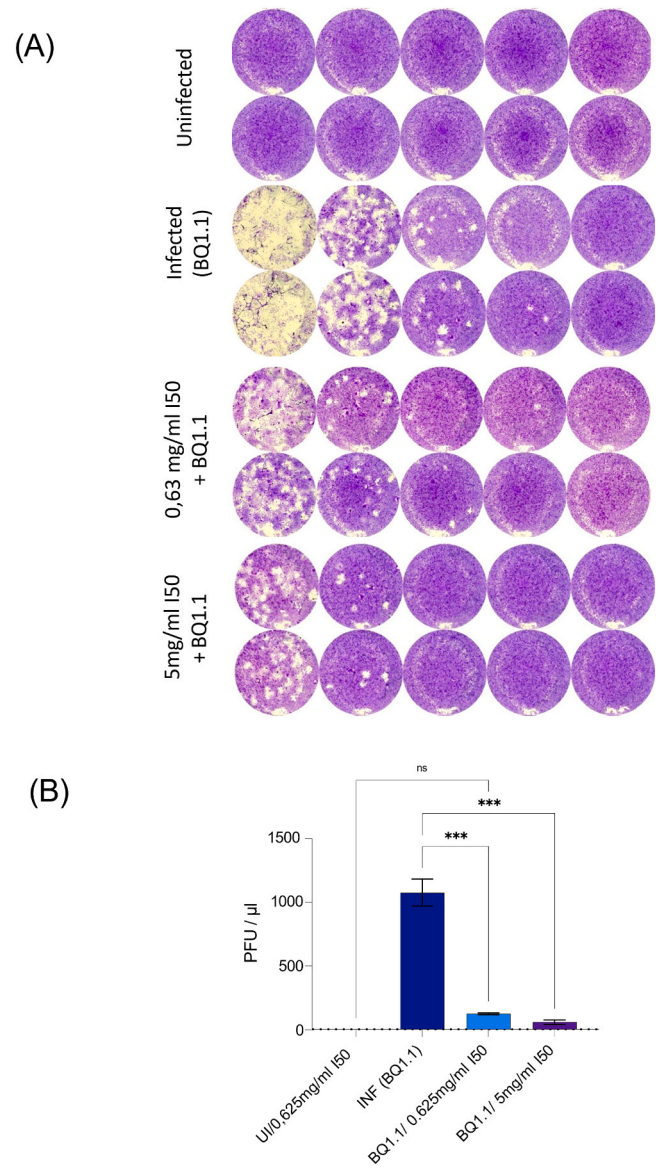

Fig. 5. Characterization of the infectivity of supernatants from I50-pretreated and infected NHBE cells by plaque assay. Supernatants from BQ1.1-infected plus/minus I50 (0.625 and 5 mg/ml)-pretreatment were applied at 3 dpi in a plaque assay. (A) shows a representative experiment performed in duplicate, while (B) is a summary of three independent experiments performed in duplicates.

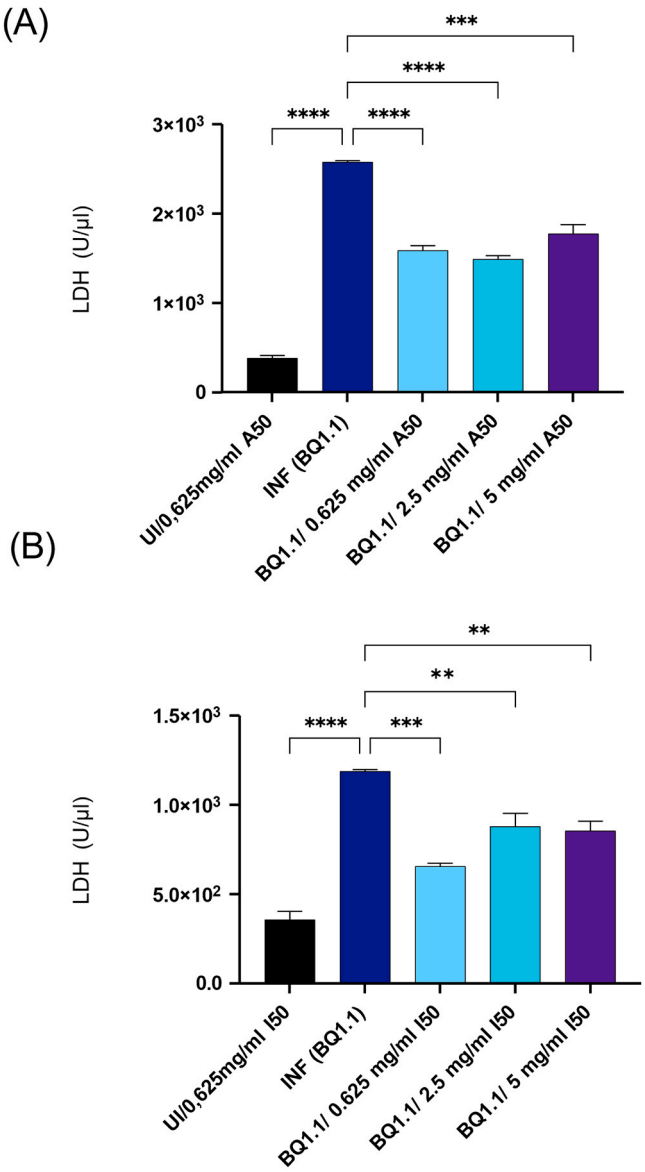

Fig. 6. Characterization of cytotoxicity following infection with BQ1.1 in absence and presence of the Aloe compounds. LDH release from NHBE cells are illustrated after treatment with A50 (A) and I50 (B) and infection with BQ1.1. A summary of 3 independent experiments using both, A50 and I50, is depicted. Differences were analyzed using One-way ANOVA and Šidák`s multiple comparisons test.

Our findings indicate that I50 is highly effective in protecting human airway epithelial tissue from SARS-CoV-2 BQ1.1–induced damage, even at the lowest concentration. Both *Aloe* compounds not only prevented tissue damage, but also reduced viral infection, infectious virus particle release and virus induced cytotoxic stress. Initial experiments with A50 in Vero cells showed a significant inhibition of SARS-CoV-2 spike protein-driven cell entry. Vero cells do not reflect several aspects of the respiratory epithelium, including the formation of tight junctions. Nevertheless, these results formed a solid basis for further evaluation of both A50 and I50 in the NHBE model, a physiologically relevant system and a primary cell in origin for testing prophylactic or therapeutic efficacy of compounds against respiratory viruses, such as SARS-CoV-2. Since the present studýs data suggest only minimal direct effect on spike proteins, but emphasizes barrier protection by APS, it is likely that the compounds act also therapeutically.

Here, the compounds were applied prior exposure to virus, and it remains interesting to evaluate, on whether the *Aloe* products could also rescue from an already established infection, thus exerting not only prophylactic, but also therapeutic potential. Moreover, we evaluated whether the Aloe compounds A50 and I50 prevent infection by maintaining epithelial barrier integrity or by directly inhibiting viral entry and replication, thereby preserving epithelial structure. Pre-incubation of viruses with varying concentrations of either A50 or I50 prior to infection resulted in only a minor reduction in viral load, suggesting a limited direct effect on viral entry and replication. The higher bioactivity of I50 compared to A50 may be attributed to its greater acetyl content likely due to differences in elution. As a result, I50 contains nearly twice the amount of acemannan as A50. Moreover, methyl group signal analysis suggests that O-acetyl groups of I50 are positioned differently than in A50. I50 is promising, since this compound exerted lower cytotoxicity and higher antiviral efficacy at low concentrations. Whether the increased *in vitro* efficacy of I50 over A50 against SARS-

CoV-2 transmission, can be attributed to it higher contents of acemannan and acetylation as shown recently by Shih et al. [28] and described in Refs [58,59], may warrant further investigation. Similarly, the host cell factor(s) engaged by the spike protein and likely targeted by these compounds for inhibition of viral entry require further investigation. In summary, both A50 as well as I50 proved highly effective in preventing the transmission of SARS-CoV-2 Omicron BQ1.1 variant in a human primary model. The *Aloe*-derived compounds restored tissue integrity, blocked viral infection in highly differentiated HAE cells, and reduced local LDH release. While these findings are based on *in vitro* data and may not directly translate to *in vivo* efficacy, these natural compounds are potential candidates for further development into inhalation forms, either to prevent or to restore alveolar epithelium against damages caused by respiratory viruses.

Contributions

WP, SAE, VZ, EP, UC, SA, SP and MH performed experiments, prepared figures and analyzed data, RB-W acquired SARS-CoV-2 patient isolates, supported drafting the manuscript and substantially revised it, EP, SP, MH supported data interpretation, drafting and revising the manuscript, WP, EP and DW designed the study, analyzed data and performed statistics, drafted the manuscript and finalized the manuscript. All authors reviewed and approved the submitted version. All authors have agreed to being accountable for their contributions and for submitting an accurate and integer work.

Ethics approval and consent to participate

Written informed consent was obtained from all donors of leftover nasopharyngeal/ oropharyngeal specimens for sampling Omicron BQ1.1. The Ethics Committee of the Medical University of Innsbruck approved the study (ECS1166/2020).

Funding

The study was in part funded by Dazzeon Biotech Co., Ltd and in part by the Austrian Science Fund (FWF) [Grant DOI:10.55776/P34070 to W.P]. The funders did not have any influence on the study and data acquisition and analyses. For open access purposes, the author has applied a CC BY public copyright license to any author accepted manuscript version arising from this submission.

CRediT authorship contribution statement

Stefan Pöhlmann: Writing – review & editing, Methodology, Investigation, Data curation. **Singh Anuma:** Writing – review & editing, Resources. **Markus Hoffmann:** Writing – review & editing, Methodology, Investigation, Data curation. **Viktoria Zaderer:** Writing – review & editing, Methodology, Investigation, Data curation. **Sophie Ann Erckert:** Methodology, Software, Validation, Writing – review & editing. **Ekambaranellore Prakash:** Writing – review & editing, Resources, Project administration, Funding acquisition, Conceptualization. **Uvarani Chokkalingam:** Writing – review & editing, Resources. **Rosa Bellmann-Weiler:** Writing – review & editing, Validation, Resources. **Doris Wilflingseder:** Writing – review & editing, Writing – original draft, Visualization, Validation, Supervision, Project administration, Methodology, Funding acquisition, Data curation, Conceptualization. **Wilfried Posch:** Writing – review & editing, Writing – original draft, Validation, Project administration, Funding acquisition, Data curation, Conceptualization.

Consent for publication

Not applicable.

Declaration of Competing Interest

The authors declare the following financial interests/personal relationships which may be considered as potential competing interests. The study was in part funded by Dazzeon and in part by the Austrian Science Fund (FWF) [Grant DOI:10.55776/P34070 to W.P]. The funders did not have any influence on the study and data acquisition and analyses. For open access purposes, the author has applied a CC BY public copyright license to any author accepted manuscript version arising from this submission. Ekamballore Prakash was previously affiliated with Dazzeon Biotechnology as Director-Botanical Development and Applications. However, this affiliation did not have any influence on the study, data acquisition and analyses and manuscript preparation.

Acknowledgements

We thank our technicians Karolin Thurnes and Christina Witting for their valuable support regarding this manuscript.

Appendix A. Supporting information

Supplementary data associated with this article can be found in the online version at doi:10.1016/j.biopha.2025.118657.

Data availability

No big data were generated within the work and all data are included in the manuscript.

References

[1] R.J. Hewitt, C.M. Lloyd, Regulation of immune responses by the airway epithelial cell landscape, Nat. Rev. Immunol. 21 (6) (2021) 347–362.
[2] O. Kayalar, et al., Impact of particulate air pollution on airway injury and epithelial plasticity; underlying mechanisms, Front Immunol. 15 (2024) 1324552.
[3] M.J. Holtzman, et al., The role of airway epithelial cells and innate immune cells in chronic respiratory disease, Nat. Rev. Immunol. 14 (10) (2014) 686–698.
[4] R.J. Russell, et al., The airway epithelium: an orchestrator of inflammation, a key structural barrier and a therapeutic target in severe asthma, Eur. Respir. J. (2024).
[5] H. Guo-Parke, et al., Deciphering Respiratory-Virus-Associated interferon signaling in COPD airway epithelium, Med. (Kaunas.) 58 (1) (2022).
[6] M.E. Love, D. Proud, Respiratory viral and bacterial exacerbations of COPD-The role of the airway epithelium, Cells 11 (9) (2022).
[7] C.A. Pollard, M.P. Morran, A.L. Nestor-Kalinoski, The COVID-19 pandemic: a global health crisis, Physiol. Genom. 52 (11) (2020) 549–557.
[8] M. Salehi-Vaziri, et al., The ins and outs of SARS-CoV-2 variants of concern (VOCs), Arch. Virol. 167 (2) (2022) 327–344.
[9] S. DeWolf, et al., SARS-CoV-2 in immunocompromised individuals, Immunity 55 (10) (2022) 1779–1798.
[10] J. Gonzalez-Rubio, et al., SARS-CoV-2 particles promote airway epithelial differentiation and ciliation, Front Bioeng. Biotechnol. 11 (2023) 1268782.
[11] R. Robinot, M. Hubert, G. Dias de Melo, et al., SARS-CoV-2 infection induces the dedifferentiation of multiciliated cells and impairs mucociliary clearance, Nat. Commun. 12 (2021) 4354.
[12] A. Shepley-McTaggart, C.A. Sagum, I. Oliva, et al., SARS-CoV-2 envelope (E) protein interacts with PDZ-domain-2 of host tight junction protein ZO1, PLoS ONE 16 (6) (2021) e0251955.
[13] S. Deinhardt-Emmer, S. Böttcher, C. Häring, et al., SARS-CoV-2 causes severe epithelial inflammation and barrier dysfunction, J. Virol. (2021).
[14] M.M. Lamers, B.L. Haagmans, SARS-CoV-2 pathogenesis, Nat. Rev. Microbiol 20 (5) (2022) *270–284*.
[15] A. Pizzorno, et al., Interactions between severe acute respiratory syndrome coronavirus 2 replication and major respiratory viruses in human nasal epithelium, J. Infect. Dis. 226 (12) (2022) 2095–2104.
[16] S. Hao, K. Ning, C.A. Kuz, et al., SARS-CoV-2 infection of polarized human airway epithelium induces necroptosis that causes airway epithelial barrier dysfunction, J. Med Virol. 95 (9) (2023 Sep) e29076, https://doi.org/10.1002/jmv.29076. PMID: 37671751; PMCID: PMC10754389.
[17] S. Yamada, T. Noda, K. Okabe, S. Yanagida, M. Nishida, Y. Kanda, SARS-CoV-2 induces barrier damage and inflammatory responses in the human iPSC-derived intestinal epithelium, J. Pharm. Sci. 149 (3) (2022 Jul) 139–146, https://doi.org/10.1016/j.jphs.2022.04.010. Epub 2022 May 2. PMID: 35641026; PMCID: PMC9060709.
[18] X. Ji, et al., Evaluation of Calu-3 cell lines as an in vitro model to study the inhalation toxicity of flavoring extracts, Toxicol. Mech. Methods 32 (3) (2022) 171–179.

[19] V.C. George, H.P.V. Rupasinghe, Apple flavonoids suppress Carcinogen-Induced DNA damage in normal human bronchial epithelial cells, Oxid. Med Cell Longev. 2017 (2017) 1767198.
[20] K.W. Lee, et al., Protective effects of chebulic acid on alveolar epithelial damage induced by urban particulate matter, BMC Complement Alter. Med 17 (1) (2017) 373.
[21] A.O. Oriola, A.O. Oyedeji, Plant-Derived natural products as lead agents against common respiratory diseases, Molecules 27 (10) (2022).
[22] N. Lu, et al., Preventive effect of arctium lappa polysaccharides on acute lung injury through Anti-Inflammatory and antioxidant activities, Nutrients 15 (23) (2023).
[23] X. Lin, et al., Lycium barbarum polysaccharide attenuates Pseudomonas-aeruginosa pyocyanin-induced cellular injury in mice airway epithelial cells, Food Nutr. Res 66 (2022).
[24] P. Huang, et al., Plant polysaccharides with anti-lung injury effects as a potential therapeutic strategy for COVID-19, Front Pharm. 13 (2022) 982893.
[25] E. Espano, J. Kim, J.K. Kim, Utilization of aloe compounds in combatting viral diseases, Pharm. (Basel) 15 (5) (2022).
[26] Y. Bai, et al., A new biomaterial derived from aloe vera-Acemannan from basic studies to clinical application, Pharmaceutics 15 (7) (2023).
[27] F. Comas-Serra, et al., Evaluation of acemannan in different commercial beverages containing aloe vera (Aloe barbadensis Miller) gel, Gels 9 (7) (2023).
[28] P.C. Shih, et al., The aloe vera acemannan polysaccharides inhibit phthalate-induced cell viability, metastasis, and stemness in colorectal cancer cells, Ecotoxicol. Environ. Saf. 288 (2024) 117351.
[29] Dichtl, S., et al., *Cilgavimab/Tixagevimab as alternative therapeutic approach for BA.2 infections*. Front Med (Lausanne), 2022. 9: p. 1005589.
[30] P. Grubwieser, et al., Human airway epithelium controls pseudomonas aeruginosa infection via inducible nitric oxide synthase, Front Immunol. 15 (2024) 1508727.
[31] V. Zaderer, et al., P80 natural essence spray and lozenges provide respiratory protection against influenza A, B, and SARS-CoV-2, Respir. Res 25 (1) (2024) 102.
[32] S. Matsuyama, et al., Enhanced isolation of SARS-CoV-2 by TMPRSS2-expressing cells, Proc. Natl. Acad. Sci. USA 117 (13) (2020) 7001–7003.
[33] Y. Wang, et al., Repair and regeneration of the alveolar epithelium in lung injury, FASEB J. 38 (8) (2024) e23612.
[34] S. Moon, et al., Airway epithelial CD47 plays a critical role in inducing influenza virus-mediated bacterial super-infection, Nat. Commun. 15 (1) (2024) 3666.
[35] L.V. Generalova, et al., Evaluation of the polysaccharide "immeran" activity in Syrian hamsters' model of SARS-CoV-2, Viruses 16 (3) (2024).
[36] C.Y. Lee, et al., Repurposing astragalus polysaccharide PG2 for inhibiting ACE2 and SARS-CoV-2 spike syncytial formation and Anti-Inflammatory effects, Viruses 15 (3) (2023).
[37] Y. You, et al., Structural characterization and SARS-CoV-2 inhibitory activity of a sulfated polysaccharide from caulerpa lentillifera, Carbohydr. Polym. 280 (2022) 119006.
[38] J. Zhang, et al., Ginseng polysaccharide enhances the humoral and cellular immune responses to SARS-CoV-2 RBD protein subunit vaccines, Vaccin. (Basel) 11 (12) (2023).
[39] Z. Sun, et al., Aloe polysaccharides inhibit influenza a virus Infection-A promising natural Anti-flu drug, Front Microbiol 9 (2018) 2338.
[40] E.D. Lewis, et al., Healthy adults supplemented with a nutraceutical formulation containing aloe vera gel, rosemary and poria cocos enhances the effect of influenza vaccination in a randomized, triple-blind, placebo-controlled trial, Front Nutr. 10 (2023) 1116634.
[41] A.O. Azghani, et al., A beta-linked mannan inhibits adherence of pseudomonas aeruginosa to human lung epithelial cells, Glycobiology 5 (1) (1995) 39–44.
[42] L. Li, et al., Aloe polymeric acemannan inhibits the cytokine storm in mouse pneumonia models by modulating macrophage metabolism, Carbohydr. Polym. 297 (2022) 120032.
[43] M.E. Abouelela, et al., Identification of potential SARS-CoV-2 main protease and spike protein inhibitors from the genus aloe: an in silico study for drug development, Molecules 26 (6) (2021).
[44] P.T. Mpiana, et al., Identification of potential inhibitors of SARS-CoV-2 main protease from aloe vera compounds: a molecular docking study, Chem. Phys. Lett. 754 (2020) 137751.
[45] D. Bohan, et al., Phosphatidylserine receptors enhance SARS-CoV-2 infection, PLoS Pathog. 17 (11) (2021) e1009743.
[46] T.M. Clausen, et al., SARS-CoV-2 infection depends on cellular heparan sulfate and ACE2, Cell 183 (4) (2020) 1043–1057, e15.
[47] G.H. Guibinga, et al., Cell surface heparan sulfate is a receptor for attachment of envelope protein-free retrovirus-like particles and VSV-G pseudotyped MLV-derived retrovirus vectors to target cells, Mol. Ther. 5 (5 Pt 1) (2002) 538–546.
[48] B. Tu, et al., Inhaled heparin polysaccharide nanodecoy against SARS-CoV-2 and variants, Acta Pharm. Sin. B 12 (7) (2022) 3187–3194.
[49] C. Pawlowski, et al., Enoxaparin is associated with lower rates of mortality than unfractionated heparin in hospitalized COVID-19 patients, EClinicalMedicine 33 (2021) 100774.
[50] J. Eder, et al., Inhalation of low molecular weight heparins as prophylaxis against SARS-CoV-2, mBio 13 (6) (2022) e0255822.
[51] I. Gouin-Thibault, E. Pautas, V. Siguret, Safety profile of different low-molecular weight heparins used at therapeutic dose, Drug Saf. 28 (4) (2005) 333–349.
[52] J.K. Shute, E. Puxeddu, L. Calzetta, Therapeutic use of heparin and derivatives beyond anticoagulation in patients with bronchial asthma or COPD, Curr. Opin. Pharm. 40 (2018) 39–45.
[53] G. Davison, et al., ColdZyme(R) reduces viral load and upper respiratory tract infection duration and protects airway epithelia from infection with human rhinoviruses, J. Physiol. 603 (6) (2025) 1483–1501.
[54] V. Zaderer, et al., GlyPerA effectively shields airway epithelia from SARS-CoV-2 infection and inflammatory events, Respir. Res 24 (1) (2023) 88.
[55] V. Zaderer, et al., ColdZyme(R) protects airway epithelia from infection with BA.4/5, Respir. Res 23 (1) (2022) 300.
[56] V. Zaderer, et al., P80 natural essence exerts efficient Anti-HIV-1- as well as adjuvant effects in DCs, Vaccin. (Basel) 9 (9) (2021).
[57] W. Posch, et al., ColdZyme maintains integrity in SARS-CoV-2-Infected airway epithelia, mBio 12 (2) (2021).
[58] J. Chokboribal, et al., Deacetylation affects the physical properties and bioactivity of acemannan, an extracted polysaccharide from aloe vera, Carbohydr. Polym. 133 (2015) 556–566.
[59] S. Kumar, R. Kumar, Role of acemannan O-acetyl group in murine radioprotection, Carbohydr. Polym. 207 (2019) 460–470.